A Test of the Validity of Cumulus Cloud Parameterizations for Longwave Radiation Calculations

D. Han and R. G. Ellingson
Department of Meteorology
University of Maryland
College Park, Maryland

Introduction

Longwave radiative transfer under broken cloud conditions is primarily a problem in cloud bulk geometry for liquid water cumulus clouds because individual clouds are nearly black. However, climate models ignore cloud geometry and approximate broken clouds as black plates. Several groups have adopted the simplicity of the flat plate approximation and have extended it to include cloud geometry and scattering by defining an effective cloud fraction that depends upon observable, bulk cloud parameters. However, these approximations have not been tested against observations. In this study, ground-based measurements at the Atmospheric Radiation Measurement (ARM) Program Cloud and Radiation Testbed (CART) site in Oklahoma are used to derive the effective cloud cover, actual cloud cover, and many other variables characterizing cumulus clouds. Different parameterizations for cumulus cloud effective cloud fraction are tested by comparing effective amounts derived from hemispheric flux observations with observed cloud cover and values predicted by the parameterizations.

Cumulus Cloud Parameterizations

Longwave radiative quantities such as radiances, fluxes, and cooling rates are often calculated as the cloud amount weighted average of the values for homogeneous clear and cloudy conditions. For example, longwave fluxes in most general circulation models (GCMs) are calculated in the form

$$F = (1-N)\,F_c + N\,F_o$$

where N is the absolute fraction of flat plate clouds, F_c and F_o are the fluxes that would occur if the sky were clear or completely covered by a single cloud layer of uniform optical properties. However, under cumulus cloud conditions, cloud sides may obscure part of the clear sky fraction if viewing at a non-zero angle. A small disparity in cloud cover can significantly alter the gradient and/or magnitude of longwave radiative properties, which may in turn affect the cloud evolution and life span and ultimately influence the climate study (Han and Ellingson 1997).

A practical and time-saving approach to account for the effect of cumulus clouds in a one-dimensional scheme is to adopt the effective cloud fraction, N_e, instead of N. N_e is the absolute cloud fraction required to generate the correct longwave radiative properties for the assumptions made concerning cumulus clouds. If one neglects the scattering by cumulus clouds, the form of the dependence of N_e on cumulus cloud parameters may be described as a function of N, cloud thickness h, aspect ratio β (defined as the ratio of h to radius for a cylinder and the ratio of h to half side length for a cuboidal, respectively), cloud non-isothermality factor, cloud base height Z_b, and exponents governing the cloud spatial and size distributions. The complexity of parameterizations determines the combination of cloud parameters.

In this study, we selected the fractal cuboidal/cylinder model (Han and Ellingson 1997), random cylinder model (Ellingson 1982), regular cuboidal model (Harshvandhan and Weinman 1982), and shifted-periodic array cuboidal model (Naber and Weinman 1984) to calculate N_e in terms of observed cloud variables from the central facility of the ARM Southern Great Plains (SGP) CART site. Comparisons among these models are shown in Figure 1.

Derivation of Cloud Variables

In order to assure the quality of the validation of the cumulus cloud parameterizations, this study is restricted to occurrences of single-layer cumulus cloud fields. Observations from a whole sky imager (WSI), a micropulse lidar (MPL), and a ceilometer were used to distinguish single-layer cumulus cloud fields from others. Using an empirically determined optimum sampling period of 10 minutes (Han 1996), we extracted the effective cloud fraction N_e from measurements by a pyrgeometer and the Atmospheric Emitted Radiance

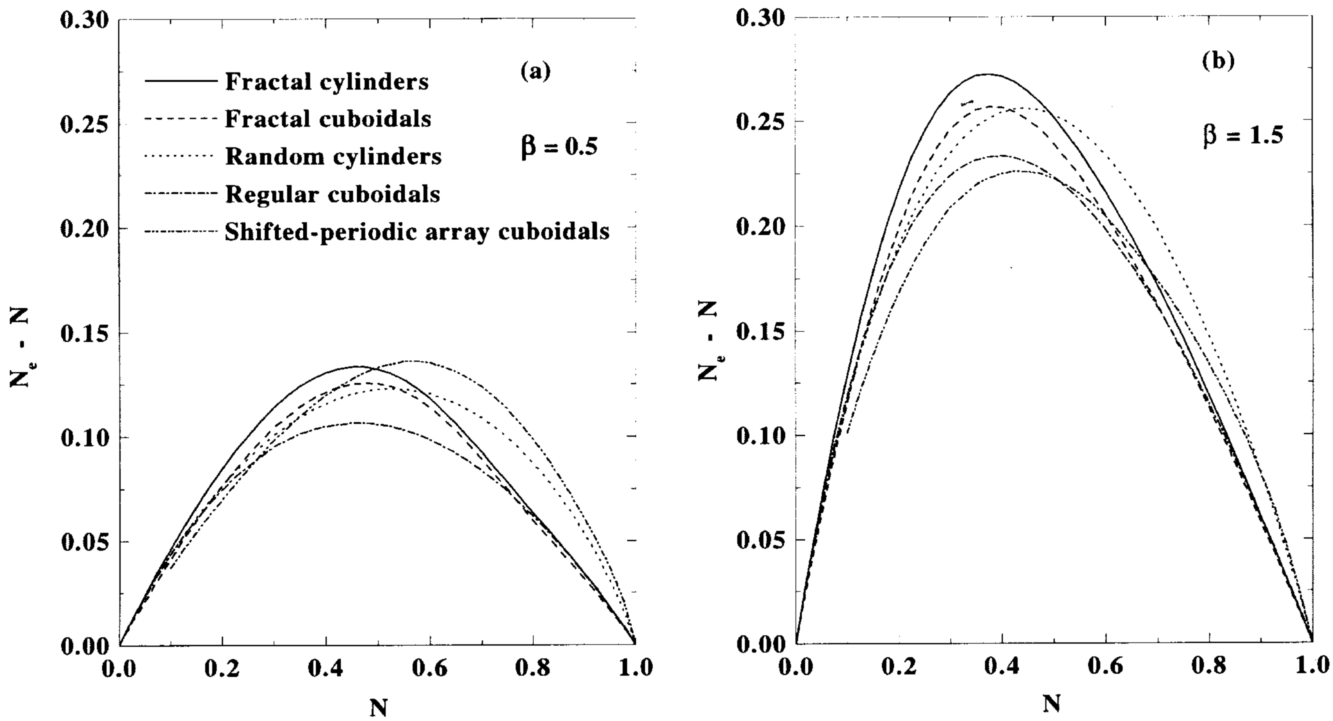

Figure 1. Comparisons among the selected cloud models with the cloud aspect ratios taking values of (a) β = 0.5 and (b) β = 1.5, respectively.

Interferometer (AERI), and determined the effective cloud radius/side length and the absolute cloud fraction from ceilometer and radiosonde data.

We would like to have obtained the distribution of cloud base and top heights simultaneously with the other measurements. Such data would be possible with a scanning millimeter cloud radar or a cloud-profiling radar, but these were not available. Instead, we used radiosonde temperature and moisture soundings (once every 3 hours) to determine the average cloud top height during the period. With the cloud base height detected by the ceilometer, we estimated the average cloud thickness and, further, the cumulus cloud aspect ratio. The non-isothermality factor was calculated with a radiation model.

There were no direct observations involving the cloud spatial and size distributions over the central facility site. Therefore, the exponents governing the cloud spatial and size distributions were adopted from other studies that used analyses of Landsat Multispectral Scanner imagery (e.g., Joseph and Cahalan 1990; Sengupta et al. 1990; and Zhu et al. 1992). In the calculations of N_e, these two exponents were assigned values of 2.5 and 2.0, respectively.

Overall, 436 single-layer cumulus cloud cases were obtained from the observations during the time period of May-July 1994. Figure 2 illustrates the distribution of N_e - N

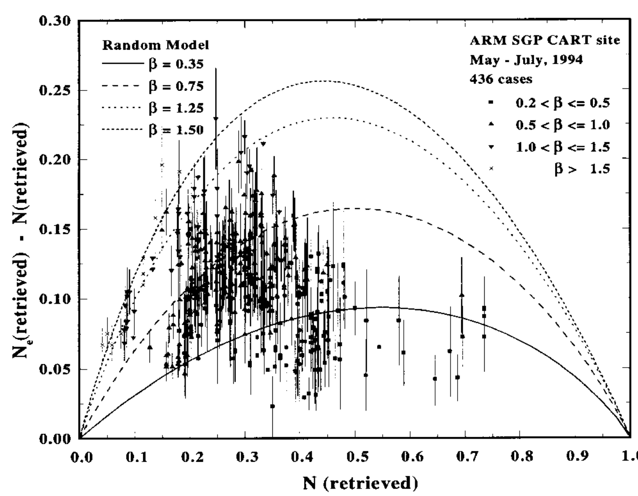

Figure 2. The distribution of N_e - N as a function of N and β from 436 cases of single-layer cumulus clouds. Half of each vertical bar indicates the standard deviation of uncertainty in retrieved N_e.

retrieved from the data for different aspect ratios. The solid lines show the results from the random cylinder model calculations. The majority of the cases have β's in the range of 0.25 to 1.25 and N's varying from 0.1 to 0.5. The relationship between the retrieved N_e and N indicates that the effect of bulk geometry of cumulus clouds does make N_e significantly different from the flat plate cloud coverage.

Validation of Cloud Parameterizations

To test the validity of the selected cumulus cloud parameterizations, N_e was calculated for each model tested using observed cloud variables as input. Realizing the uncertainties involved in the cloud variables, we also tested the sensitivity of models to each cloud variable. Shown in Figure 3 are examples of the various tests for the random cylinder model.

Within the test range, the random cylinder model agrees well with the observations. The 75th and 95th percentiles of the model relative accuracy, defined as the ratio of the difference between the calculated and retrieved N_e's to the retrieved N_e, reach 5.1% and 11%, respectively. On the other hand, the sensitivity test indicates that it is necessary to perform more accurate as well as more comprehensive measurements for clouds. As implied in Figure 3(b), a

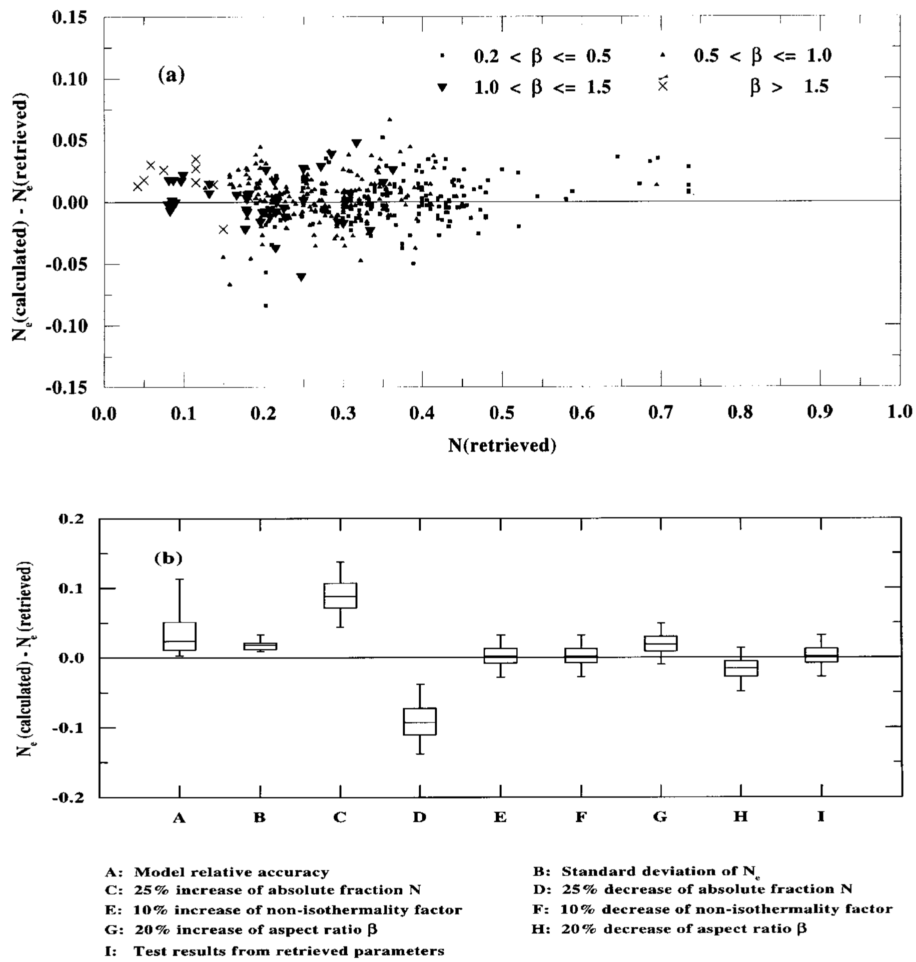

Figure 3. Tests of the random cylinder model: (a) the distribution of the differences between the calculated and retrieved effective cloud fractions, and (b) box plots showing the relative accuracies of the model and the sensitivity of the model to each cloud parameter.

variation in determining β and N due to insufficient observations may affect the validation.

Similar tests were conducted for the other models and the results are summarized in Figure 4 and Table 1. The results indicate that, except for the fractal cylinder model, the other models achieve a mean relative accuracy of about 4% and their relative accuracies at the 75th and 95th percentiles are about 5.5% and 12%, respectively.

Conclusion

This is the first validation of the form of the dependence of the effective cloud fraction on bulk cloud parameters using independently measured data at the surface. However, this test does not lead to a conclusion concerning the best model for cumulus clouds. We did not have concurrent observations of the cloud spatial and size distributions, both of which influence the calculation of N_e (Han and Ellingson 1997). Additionally, there were few cases in the range of greatest sensitivity with large β and N, in which model comparisons demonstrate larger disparity.

Nevertheless, the ground-based measurements, being operated at the ARM SGP, TWP (Tropical Western Pacific) and NSA (North Slope of Alaska) sites, will allow one to collect a large diversity of finite cumulus cloud fields. Cloud radars, being deployed by the ARM Program, will provide more accurate

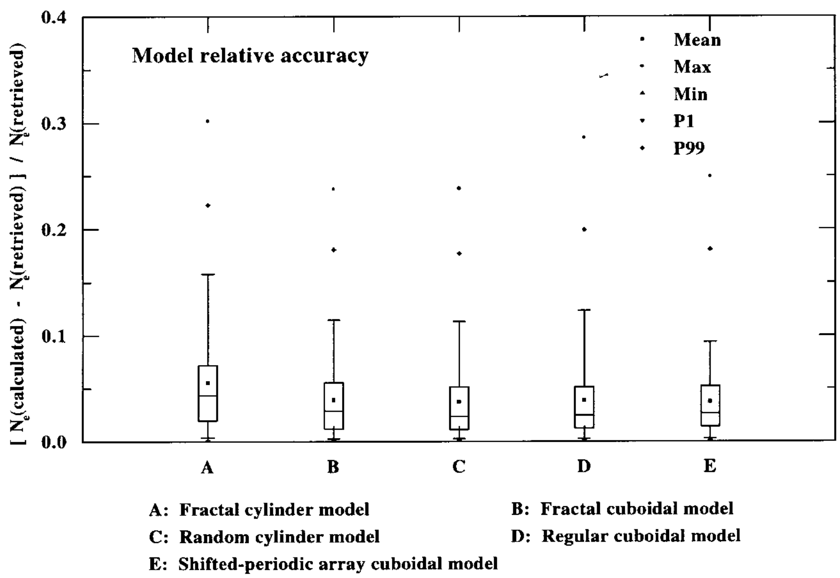

Figure 4. The distributions of the relative accuracies of the tested models.

Table 1. Summary of cloud model tests.

	Relative accuracy		Relative accuracy achieved at the	
	Mean	Standard deviation	75th percentile	95th percentile
Fractal cylinders	5.5%	4.8%	7.2%	16%
Fractal cuboidals	3.9%	3.8%	5.5%	12%
Random cylinders	3.7%	3.8%	5.1%	11%
Regular cuboidals	3.9%	4.0%	5.1%	12%
Shifted-periodic	3.8%	3.5%	5.2%	9.1%

determination of many cloud variables. Extensions of the tests described herein with the new data should lead to an optimization of current cumulus cloud parameterizations for longwave radiation calculations.

Acknowledgments

This research was supported by the U.S. Department of Energy Grant DEFG0294ER61746 and the University of Maryland.

References

Ellingson, R. G., 1982: On the effects of cumulus dimensions on longwave irradiance and heating rate calculations. *J. Atmos. Sci.*, **39**, 886-896.

Han, D., 1996: *Studies of longwave radiative transfer under broken cloud conditions: Cloud parameterizations and validations.* Dissertation, Department of Meteorology, University of Maryland, College Park, Maryland.

Han, D., and R. G. Ellingson, 1997: Cumulus cloud parameterizations for longwave radiation calculations. *J. Atmos. Sci*., submitted.

Harshvandhan, and J. A. Weinman, 1982: Infrared radiative transfer through a regular array of cuboidal clouds. *J. Atmos. Sci*., **39**, 431-439.

Joseph, J. H., and R. F. Cahalan, 1990: Nearest neighbor spacing of fair weather cumulus clouds. *J. Appl. Meteor*., **29**, 793-805.

Naber, P. S., and J. A. Weinman, 1984: The angular distribution of infrared radiances emerging from broken fields of cumulus clouds. *J. Geophys. Res*., **89**, 1249-1257.

Sengupta, S. K., R. M. Welch, M. S. Navar, T. A. Berendes, and D. W. Chen, 1990: Cumulus cloud field morphology and spatial patterns derived from high spatial resolution Landsat imagery. *J. Appl. Meteor*., **29**, 1245-1267.

Zhu, T., J. Lee, R. C. Weger, and R. M. Welch, 1992: Clustering, randomness, and regularity in cloud fields: 2. Cumulus cloud fields. *J. Geophys. Res.*, **97**, 20537-20558.